



Zinc Oxide Nanoparticles Trigger Autophagy in the Human Multiple Myeloma Cell Line RPMI8226: an In Vitro Study

Zonghong Li¹ · Xuewei Yin¹ · Chunyi Lyu¹ · Jingyi Wang² · Kui Liu² · Siyuan Cui² · Shumin Ding² · Yingying Wang² · Jinxin Wang² · Dadong Guo³ · Ruirong Xu^{2,4,5}

Received: 6 May 2023 / Accepted: 18 June 2023

© The Author(s), under exclusive licence to Springer Science+Business Media, LLC, part of Springer Nature 2023

Abstract

Multiple myeloma (MM) is a malignant clonal proliferative plasma cell tumor. Zinc oxide nanoparticles (ZnO NPs) are used for antibacterial and antitumor applications in the biomedical field. This study investigated the autophagy-induced effects of ZnO NPs on the MM cell line RPMI8226 and the underlying mechanism. After RPMI8226 cells were exposed to various concentrations of ZnO NPs, the cell survival rate, morphological changes, lactate dehydrogenase (LDH) levels, cell cycle arrest, and autophagic vacuoles were monitored. Moreover, we investigated the expression of Beclin 1 (Becn1), autophagy-related gene 5 (Atg5), and Atg12 at the mRNA and protein levels, as well as the level of light chain 3 (LC3). The results showed that ZnO NPs could effectively inhibit the proliferation and promote the death of RPMI8226 cells in vitro in a dose- and time-dependent manner. ZnO NPs increased LDH levels, enhanced monodansylcadaverine (MDC) fluorescence intensity, and induced cell cycle arrest at the G2/M phases in RPMI8226 cells. Moreover, ZnO NPs significantly increased the expression of Becn1, Atg5, and Atg12 at the mRNA and protein levels and stimulated the production of LC3. We further validated the results using the autophagy inhibitor 3-methyladenine (3-MA). Overall, we observed that ZnO NPs can trigger autophagy signaling in RPMI8226 cells, which may be a potential therapeutic approach for MM.

Keywords Autophagy · Multiple myeloma · Zinc oxide nanoparticles · LC3 · Atg5 · Atg12

Abbreviations

MM	Multiple myeloma
ZnO NPs	Zinc oxide nanoparticles
LDH	Lactate dehydrogenase
Becn1	Beclin 1
Atg5	Autophagy-related gene 5
LC3	Light chain 3
MDC	Monodansylcadaverine
3-MA	3-Methyladenine
PC	Plasma cells
BM	Bone marrow
TEM	Transmission electron microscope

XRD	X-ray diffraction
ANOVA	Analysis of variance
PBMCs	Peripheral blood mononuclear cells

Introduction

Multiple myeloma (MM) is a hematological malignancy characterized by malignant plasma cells (PC) proliferating abnormally in the bone marrow (BM), as well as kidney damage, bone destruction, and paraproteinemia [1, 2]. MM ranks second in the occurrence of hematological tumors [3, 4]. In recent years, the therapy of MM has improved significantly, as has the introduction of novel medications, including lenalidomide and thalidomide (an immunomodulatory drug), bortezomib (a proteasome inhibitor), and daratumumab (a monoclonal antibody). Despite the fact that these advancements have increased response rates and survival rates dramatically, these patients still have a median survival rate of 5–6 years [5, 6]. At present, MM remains an incurable hematological malignancy, and drug treatment continues to face the challenges of drug resistance and side

Zonghong Li and Xuewei Yin contributed equally to this work and share first authorship

Highlights 1. ZnO NPs effectively inhibited the proliferation of human MM RPMI8226 cells in vitro.
2. ZnO NPs enhanced Becn1, Atg5, Atg12, and LC3 expression in human MM RPMI8226 cells.
3. ZnO NPs trigger the autophagy signaling pathway in human MM RPMI8226 cells.

Extended author information available on the last page of the article

effects [7–11]. The literature reports that most patients with relapsed refractory MM have a survival of less than 12 months [12]. In addition, the treatment of MM is expensive (lenalidomide costs over \$200,000 for 1 year of treatment), and introducing these agents earlier in the disease course will impose significant costs on society and increase the burden of treatment [13]. Therefore, overcoming MM cell drug resistance and generating low-toxicity, high-efficiency agents are critical tasks in MM therapy research.

Nanoparticles (NPs) are defined as particles with at least one dimension less than 100 nm. In recent years, studies have demonstrated that NPs can overcome multidrug resistance in cancer cells [14]. Metal oxide NPs are an attractive class of NPs because of their potential cytotoxicity due to their uptake by cancer cells [15, 16]. Remarkably, zinc oxide (ZnO) NPs, FDA-approved pharmaceutical formulations with safety, stability, and biocompatibility characteristics, are widely used in industrial products and pharmaceutical formulations [17, 18]. As a result, ZnO NPs are attracting attention for their significance in biological fields, such as cancer treatment [19], antidiabetics [20], and antibacterial compounds [21], and numerous studies have also demonstrated that ZnO NPs exhibit promising antitumor activity against many kinds of human cancer cell lines while showing less toxicity for normal cells [15, 22, 23]. Our previous research indicated that ZnO NPs can effectively induce MM cell apoptosis via reactive oxygen species and the caspase signaling pathway *in vitro* [24].

Autophagy is a self-repair mechanism that degrades misfolded proteins or impaired organelles, leading to recycling. It enables cells to adapt to changes and stimuli in their surroundings, thus effectively maintaining intracellular homeostasis [25]. The process of autophagy consists of three basic stages: autophagosome production, autophagosome-lysosome fusion, and phagocytic material degradation in lysosomes [26]. However, sustained and excessive autophagy could lead to cell death due to an imbalance in intracellular homeostasis [27, 28]. Nanomaterials, regarded by cells as foreign substances, are a new class of autophagy inducers that can determine cell fate by triggering cells to undergo autophagy. In addition, cancer cell death induced by ZnO NPs has been related to the regulation of autophagy [29, 30]. Liu et al. found that ZnO NPs triggered lysosomal autophagy system alterations in rat pheochromocytoma cells, with the lysosomal and microtubule systems being notably involved [31]. Guo et al. reported that ZnO NPs could effectively inhibit tenon fibroblast proliferation by activating the autophagic signaling pathway [32]. He et al. demonstrated that ZnO NPs can mediate osteosarcoma cell death through the interaction between two mechanisms, autophagy and apoptosis [33]. Although ZnO NPs have the potential to trigger autophagy in many cells, their impact on MM cells remains unclear.

In the present study, we evaluated, for the first time, the autophagy-activating effects of ZnO NPs on MM using the human MM cell line RPMI8226. We found that ZnO NPs could effectively inhibit the proliferation and promote the death of RPMI8226 cells *in vitro* in a dose- and time-dependent manner. ZnO NPs effectively elevated LDH levels, enhanced monodansylcadaverine (MDC) fluorescence intensity, and induced cell cycle arrest at the G2/M phases in RPMI8226 cells. Moreover, ZnO NPs also significantly increased the expression of Becn1, Atg5, Atg12, and LC3 and hence triggered the autophagy signaling pathway. We also validated the results using the autophagy inhibitor 3-methyladenine (3-MA). Based on our results, there is a close relationship between ZnO NPs-induced MM cell death and the activation of autophagic signaling.

Materials and Methods

Zinc Oxide Nanoparticles (ZnO NPs) and ZnO NPs Solutions

ZnO NPs were purchased from Jiangsu Changtai Nanometer Material Co., Ltd., and the purity was not less than 99.9%. The diameter, morphology, and distribution of ZnO NPs were characterized using a transmission electron microscope (TEM; JEM2000EX, Japan) and a field emission scanning electron microscope (SEM; Zeiss Supra55, Germany) [34]. The dynamic light scattering nanoparticle analyzer (DLS; Malvern Nano-ZS, Britain) was used to determine the particle size distribution and the polydispersity index (PDI) of ZnO NPs in ethanol medium (40 µg/mL). An X-ray diffractometer (XRD; Rigaku, Tokyo, Japan) was used to determine the crystalline nature of ZnO NPs. ZnO NPs were dissolved in RPMI 1640 medium and sonicated on ice for 10 min prior to use to reduce aggregation.

Cells and Cell Culture

The human MM cell line RPMI8226 (purchased from ATCC, USA) was maintained in RPMI 1640 (Gibco BRL) containing 10% fetal bovine serum (Sigma, USA), 100 U/mL penicillin, and 100 µg/mL streptomycin. All cells were cultured in a 37 °C incubator with a 5% CO₂ humidified atmosphere [35]. An automatic cell counter (Muse; Merck Millipore, USA) was used to perform cell counts.

Cell Viability Assay

The MTT colorimetric experiment was used to detect viable cell numbers [36]. The RPMI8226 cells within five passage generations were used for the detection. Briefly, logarithmic growth stage RPMI8226 cells (density 1.0×10^5 /mL)

were added to 96-well plates (Beyotime Biotechnology, China) with 100 μ L of cell solution in each well. In addition, dilute solutions of different concentrations (final concentrations were 0, 2.5, 5.0, 10.0, 20.0, 40.0, and 60.0 μ g/mL) of ZnO NPs were added to each well. Then, the cells were cultured in a sterile incubator at 37 °C for 24, 48, and 72 h. At the appointed time, 20 μ L of MTT (5 mg/mL) was added to each well and incubated in the incubator for an additional 4 h. Finally, the supernatant was discarded, and 150 μ L DMSO was added. The dish was gently stirred until the blue formazan crystals were completely dissolved. After agitation, a flat plate microreader (Tecan Spectrum, Switzerland) was used to measure the absorption of the cells at 490 nm. Furthermore, the half maximal inhibitory concentration (IC_{50}) was the concentration of ZnO NPs required to inhibit the growth of RPMI8226 cells by 50% [37]. The IC_{50} was calculated via nonlinear regression in GraphPad Prism (GraphPad, La Jolla, CA, USA).

Cell Morphology

RPMI8226 cells (1.2×10^5 per well) were incubated in 6-well plates, and then various concentrations (0, 5.0, 10.0, or 20.0 μ g/mL) of ZnO NPs were added and incubated in an incubator for 24 h. At the indicated times, a light field microscope (Olympus IX71, Japan) was used to observe the morphological changes in the cells.

Lactate Dehydrogenase (LDH) Activity Assay

In this study, the LDH levels in the extracellular medium were assessed using an LDH Assay Kit (Solarbio Science & Technology Co., Ltd, China). Briefly, RPMI8226 cells were seeded in six-well plates (NEST, Biotech., Wuxi, China) at a density of 5.0×10^5 cells/well for 24 h. The cells were divided into six groups: a control group, a 5.0 μ g/mL ZnO NPs group, a 10.0 μ g/mL ZnO NPs group, a 20.0 μ g/mL ZnO NPs group, a 5 mM 3-MA group, and a ZnO NPs (20.0 μ g/mL) + 3-MA (5 mM) group. At the indicated time, the cells were collected and sonicated on ice for 15 min and centrifuged at 8000 g at 4 °C for 10 min, and then the supernatants were collected. Finally, the LDH levels were determined using supernatants. All processes were carried out according to the instructions provided by the manufacturer [38]. The absorbance at 450 nm was measured by a Multi-Mode Microplate Reader (Envision, Perkin Elmer, Waltham, MA, USA).

Cell Cycle Arrest

The cell cycle arrest of RPMI8226 cells after exposure to ZnO NPs was detected by flow cytometry. For the measurement, approximately 1.2×10^5 RPMI8226 cells

were exposed to various concentrations (0, 5.0, 10.0, and 20.0 μ g/mL) of ZnO NPs and incubated in six-well plates for 24 h. After incubation, the cells were collected, washed twice with $1 \times$ PBS, fixed in ice-cold ethanol (70%), and stored in a -20 °C refrigerator overnight. Subsequently, stored cells were rewashed with PBS and stained with ethidium bromide for final analysis by flow cytometry (Accuri C6, Michigan, USA) [39].

Monodansylcadaverine (MDC) Staining

The number of autophagic vacuoles in RPMI8226 cells was assessed by monodansylcadaverine (MDC) staining. Briefly, various concentrations (0, 5.0, 10.0, or 20.0 μ g/mL) of ZnO NPs, 5 mM 3-MA, and ZnO NPs (20.0 μ g/mL) + 3-MA (5 mM) were applied to RPMI8226 cells cultivated on 6-well culture plates for 24 h, followed by incubation with MDC solution at 37 °C for 30 min. Finally, representative images were captured using a fluorescence microscope (IX71; Olympus Corporation, Tokyo, Japan) [40].

Real-Time Quantitative PCR (qRT-PCR)

Four compounds (i.e., Becn1, Atg5, Atg12, LC3) were chosen to explore the role of autophagy in ZnO NPs-treated RPMI8226 cells. The mRNA levels of autophagic genes (Becn1, Atg5, Atg12, and LC3) were detected by qRT-PCR, with GAPDH as an internal control. In brief, RPMI8226 cells (1.2×10^5 per well) were treated with different concentrations (0, 5.0, 10.0, and 20.0 μ g/mL) of ZnO NPs for 12 h. Next, the cells were collected, and total RNA was extracted with an RNA Tissue/Cell Rapid Extraction Kit (Sparkjade Co., Ltd, China). Then, cDNA was synthesized by a first-strand cDNA synthesis kit (Takara, China). Finally, quantitative PCR was performed using the SPARKscript II SYBR one-step qRT PCR kit (Sparkjade Co., Ltd, China) [41]. The primers were as follows: Becn1 sense: 5'GGGGGTTGC GGTTTTCT3', antisense: 5'AGCCGCCACTGCCTCCTG T3'; Atg5 sense: 5'GGCCATCAATCGGAAACTCA3', antisense: 5'GCAGCCACAGGACGAAACA3'; Atg12 sense: 5'CCCCGGGAACAGAGGAACC3', antisense: 5'CTGGGG AAGGAGCAAAGGACTGAT3'; LC3 sense: 5'GGCCTT CTTCTGCTGGTGA3', antisense: 5'GCCGTCCTCGTC TTTCTCCTGCTC3', and GAPDH sense: 5'TGCACCACC AACTGCTTAGC 3', antisense: 5'GGCATGGACTGTGGT CATGAG 3'. The PCR program was set up as follows: 95 °C for 3 min, followed by 40 cycles at 95 °C for 5 s, 57 °C for 10 s, and 72 °C for 15 s. After normalization to the GAPDH control, the fold changes were determined using the $2^{-\Delta\Delta Ct}$ technique.

ELISA

We measured Becn1, Atg5, and Atg12 protein levels after ZnO NPs exposure in RPMI8226 cells. Briefly, RPMI8226 cells (6.0×10^5 cells per well) were exposed to different concentrations (0, 5.0, 10.0, or 20.0 $\mu\text{g/mL}$) of ZnO NPs for 24 h. Then, the cells were collected, washed twice with PBS, sonicated on ice for 15 min, and centrifuged to collect the supernatant. The Becn1, Atg5, and Atg12 protein levels in the supernatants were detected using a Human BECN1 ELISA kit (Elabscience Biotechnology Co., Ltd., China), a Human ATG5 ELISA kit (Wuhan Abebio Science Co., Ltd., China), and a Human ATG12 ELISA kit (Wuhan Colorful-Gene Biological Technology Co., Ltd., China) [42].

Determination of Light Chain 3 (LC3) Accumulation

We measured the levels of LC3 accumulation in RPMI8226 cells with the Muse™ Autophagy LC3 antibody-based kit (Merck Millipore) and Muse™ Cell Analyzer. Briefly, RPMI8226 cells were cultured in an incubator for 24 h with 0, 5.0, 10.0, or 20.0 $\mu\text{g/mL}$ ZnO NPs. At the end of the culture, the cells were collected and washed twice with cold PBS. Next, the cells were treated with the Muse Autophagy LC3 antibody kit as directed by the manufacturer's instructions and analyzed using a Muse™ Cell Analyzer [32].

Statistical Analysis

All results from three independent experiments are expressed as the mean \pm S.D. In this study, statistical analysis was carried out using SPSS 25.0 software, and a one-way analysis of variance (ANOVA) followed by Dunn's post-hoc test was performed. Statistical significance was accepted at $P < 0.05$.

Results

To explore the effect of ZnO NPs on RPMI8226 cells, we examined the cell survival rate, morphological alterations, LDH levels, cell cycle arrest, and autophagic vacuoles. Moreover, we explored the expression of Becn1, Atg5, and Atg12 at the mRNA and protein levels and the level of LC3. We further confirmed the autophagy-inducing effects of ZnO NPs on RPMI8226 cells through the autophagy inhibitor 3-MA. Based on our results, ZnO NPs can trigger autophagy signaling in RPMI8226 cells and thus inhibit human MM cell proliferation.

Characterization of ZnO NPs

Figure 1A and E show that the ZnO NPs were irregular, spherical, or lumpy in shape, with particle sizes ranging

from 20 to 60 nm. The DLS size distribution of ZnO NPs suspended in ethanol medium (40 $\mu\text{g/mL}$) is shown in Fig. 1B and C: the size distribution ranged from 700 to 1400 nm with a PDI of about 0.31, indicating that ZnO NPs are distributed in ethanol in a steady manner. The XRD pattern of ZnO NPs is shown in Fig. 1D. The 2θ angles of the diffraction peaks were located at $\sim 31.766^\circ$, 34.418° , 36.251° , 47.535° , 56.591° , 62.851° , 66.371° , 67.942° , 69.081° , 72.558° , and 76.953° for the (100), (002), (101), (102), (110), (103), (200), (112), (201), (004), and (202) planes. Furthermore, the XRD spectrum showed that there were only normal ZnO peaks, confirming the purity of the ZnO NPs. Moreover, the narrow and strong diffraction peak suggested that ZnO NPs had an optimal crystalline structure.

Cellular Viability

Figure 2 shows the inhibitory impact of ZnO NPs on the proliferation of RPMI8226 cells in a concentration- and time-dependent manner ($*P < 0.05$, $**P < 0.01$, and $***P < 0.001$ vs. relevant control samples). After treatment with ZnO NPs for 24, 48, and 72 h, RPMI8226 cell viability decreased with increasing culture time and concentration of ZnO NPs. At the same time, the results showed that high concentrations of ZnO NPs significantly reduced the survival rate of RPMI8226 cells and significantly inhibited the proliferation of MM cells. The IC_{50} values were 38.17 $\mu\text{g/mL}$ at 24 h, 32.40 $\mu\text{g/mL}$ at 48 h, and 22.99 $\mu\text{g/mL}$ at 72 h.

Change in Cell Morphology

As shown in Fig. 3A–D, we observed that the morphology of RPMI8226 cells was changed after treatment with ZnO NPs for 24 h. As the concentration of ZnO NPs increased, the number of intact RPMI8226 cells decreased, whereas the number of damaged cells increased. The damaged cells exhibited cell shrinkage, nuclear coagulation, and fragmentation, and the higher the ZnO NPs concentration, the more severe the cell morphological damage.

Elevation of Lactate Dehydrogenase (LDH) Levels

As shown in Fig. 4, after RPMI8226 cells were exposed to various concentrations (0, 5.0, 10.0, and 20.0 $\mu\text{g/mL}$, respectively) of ZnO NPs for 24 h, the LDH levels in the supernatant were elevated in a concentration-dependent manner, whereas 3-MA treatment markedly reduced the 20.0 $\mu\text{g/mL}$ ZnO NPs-induced LDH release level. We found that LDH levels in RPMI8226 cells increased from 100% to 134.112%, 182.243%, 221.028%, 128.972%, and 139.424%, in a concentration-dependent manner and were significantly different compared to the untreated cells ($**P < 0.01$ and $***P < 0.001$ vs. control samples). These results suggest that ZnO NPs

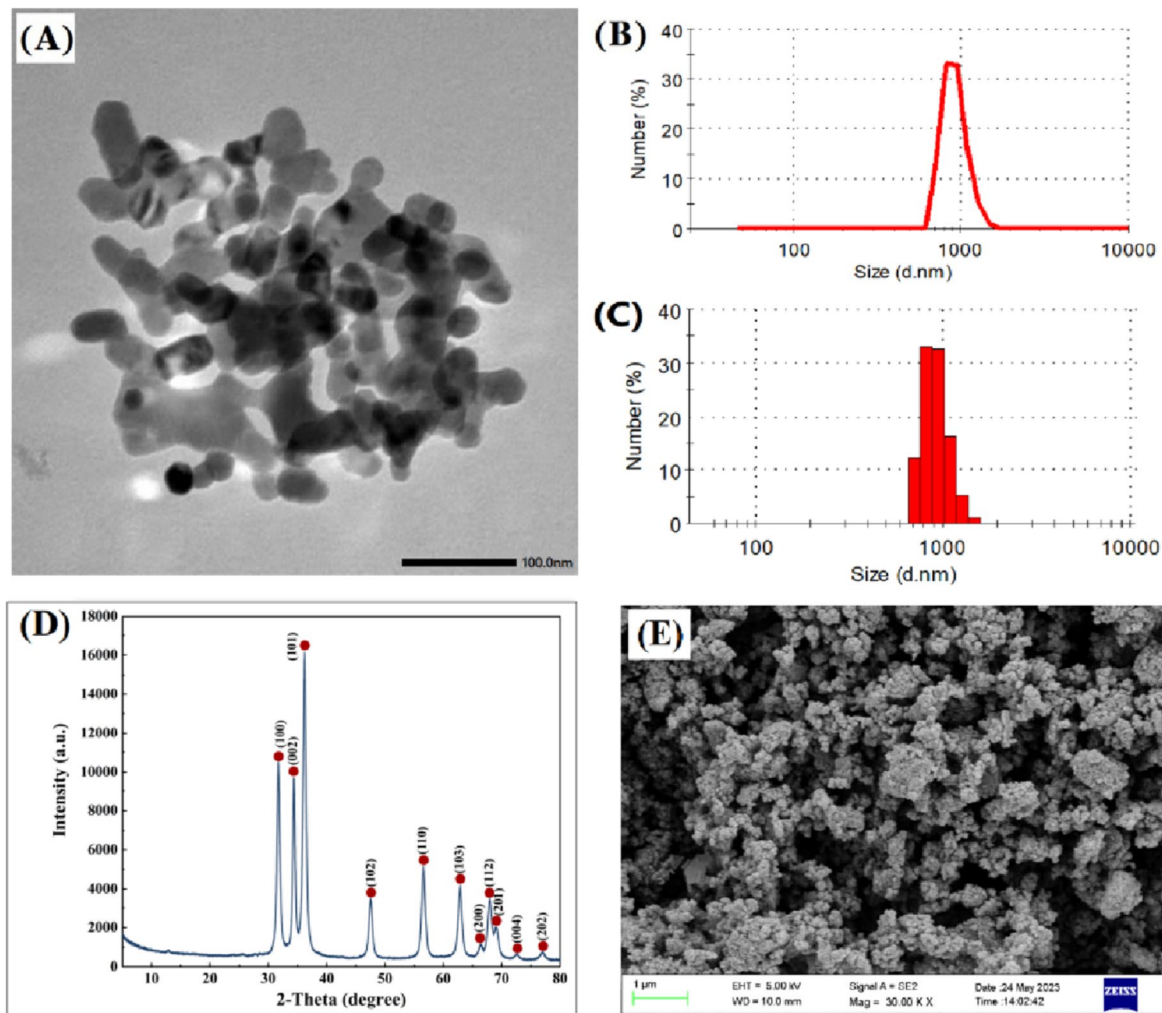


Fig. 1 Characterization of ZnO NPs. **A** Morphology of ZnO NPs characterized by transmission electron microscopy. **B** DLS of ZnO NPs suspended in ethanol medium (40 $\mu\text{g/mL}$). **C** Size distribution of

ZnO NPs suspended in ethanol medium (40 $\mu\text{g/mL}$). **D** X-ray diffraction of ZnO NPs. **E** Morphology of ZnO NPs characterized by a field emission scanning electron microscope

treatment can increase the permeability of the cytoplasmic membrane, thereby facilitating the release of LDH into the culture medium.

Cell Cycle Arrest

We evaluated the changes in cell cycle distribution after RPMI8226 cells were treated with ZnO NPs for 24 h. Figure 5 (A–E, * $P < 0.05$, ** $P < 0.01$, and *** $P < 0.001$ compared with the control group) shows that ZnO NPs caused G2/M phase cycle arrest and G0/G1 phase reduction in human MM cells. In the present study, the number of G2/M phase RPMI8226 cells increased from 22.533% to 26.500%, 29.133, and 36.900%, in a concentration-dependent manner. In contrast, the number of G0/G1 phase RPMI8226 cells decreased from 38.167% to 30.100%, 29.900%, and 22.700%, in a concentration-dependent manner. These

results indicate that ZnO NPs can induce cell cycle arrest at the G2/M phase, thereby inhibiting MM cell proliferation.

Monodansylcadaverine (MDC) Staining

MDC is a marker for autolysosomes. In the present study, MDC staining was used to investigate the abundance of autophagic vacuoles in RPMI8226 cells. In the control group, weak and diffuse MDC staining was observed throughout the cytoplasm, and very little punctate staining was observed. In ZnO NPs-treated cells, MDC staining was significantly enhanced, and the distribution pattern ranged from diffuse to punctate aggregation in a concentration-dependent manner. The punctate staining in the 3-MA + ZnO NPs treatment group was markedly reduced (Fig. 6A–F). We found that the MDC fluorescence intensity changed from 100% to 132.411%, 194.576%,

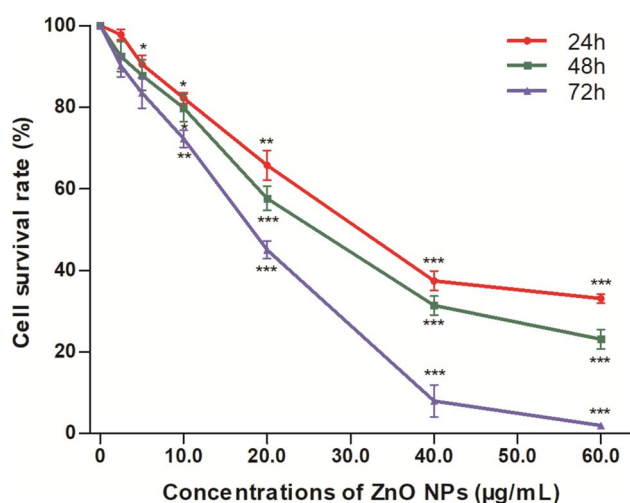


Fig. 2 Effect of different concentrations of ZnO NPs on human MM cell viability. RPMI8226 cells were incubated with different concentrations (0, 2.5, 5.0, 10.0, 20.0, 40.0, and 60.0 µg/mL) of ZnO NPs for 24 h, 48 h, and 72 h, and the cell viability was detected by MTT assay. The results are presented as the mean \pm SD of three independent experiments. * $P < 0.05$, ** $P < 0.01$, and *** $P < 0.001$

255.607%, 90.667%, and 125.000% (Fig. 6G), and there were significant differences compared to the untreated cells (* $P < 0.05$, ** $P < 0.01$, and *** $P < 0.001$ vs. control

samples). These results demonstrate that ZnO NPs triggered the autophagy process in human MM cells.

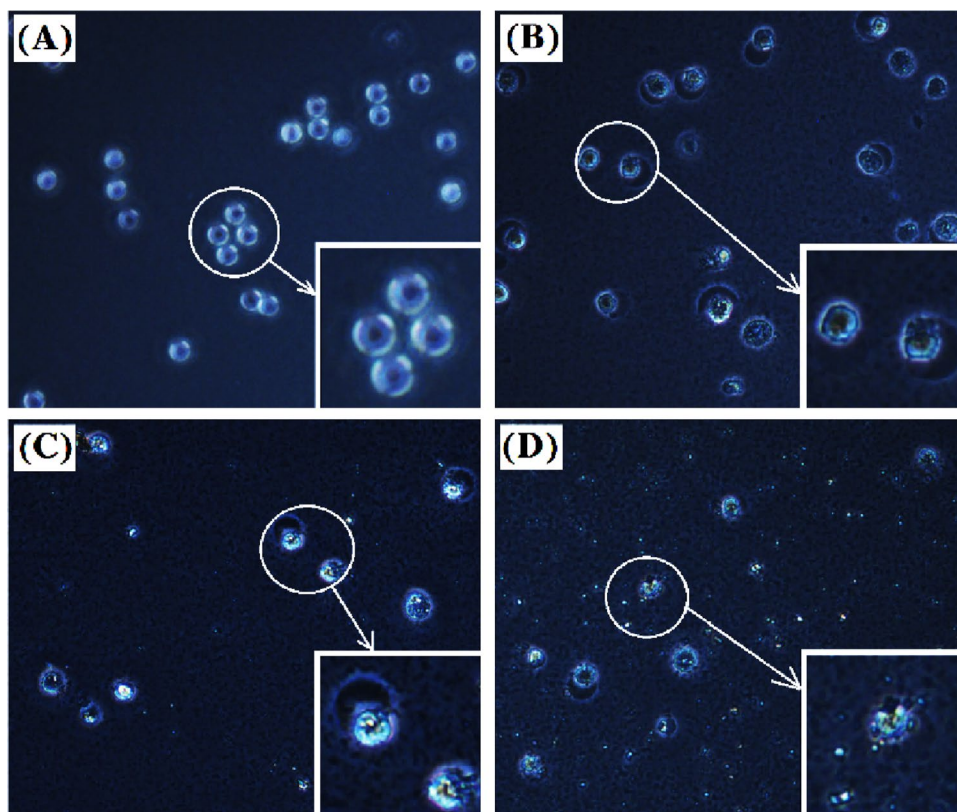
Real-Time Quantitative PCR (qRT-PCR)

Q-PCR was used to analyze the impact of varying doses of ZnO NPs on the expression of Becl1, Atg5, Atg12, and LC3. As shown in Fig. 7A–D, the levels of Becl1, Atg5, Atg12, and LC3 increased with increasing concentrations of ZnO NPs incubated with RPMI8226 cells (* $P < 0.05$, ** $P < 0.01$, and *** $P < 0.001$ vs. the control samples). We found that after exposure to various concentrations (0, 5.0, 10.0, or 20.0 µg/mL) of ZnO NPs, the mRNA level of Becl1 was elevated 1.57-, 2.82-, and 2.56-fold, respectively; the mRNA level of Atg5 was elevated 1.12-, 1.63-, and 1.89-fold; and the mRNA level of Atg12 was elevated 1.69-, 3.83- and 3.44-fold. Similarly, the LC3 mRNA levels increased 1.37-, 2.72- and 6.43-fold with concentration. These findings demonstrate a substantial difference in autophagy signaling-related protein expression between cells that were not treated (normal control) and cells that were treated with ZnO NPs.

ELISA

We further examined the changes in Becl1, Atg5, and Atg12 protein levels in RPMI8226 cells using the ELISA technique after treatment with ZnO NPs for 24 h. Figure 8A–C

Fig. 3 Morphological changes in RPMI8226 cells after exposure to different concentrations of ZnO NPs. The cells were treated with different concentrations of ZnO NPs for 24 h, and representative images were captured by a light field microscope. **A** Control cells; **B** cells exposed to 5.0 µg/mL ZnO NPs; **C** cells exposed to 10.0 µg/mL ZnO NPs; **D** cells exposed to 20.0 µg/mL ZnO NPs. Inset, magnified cells



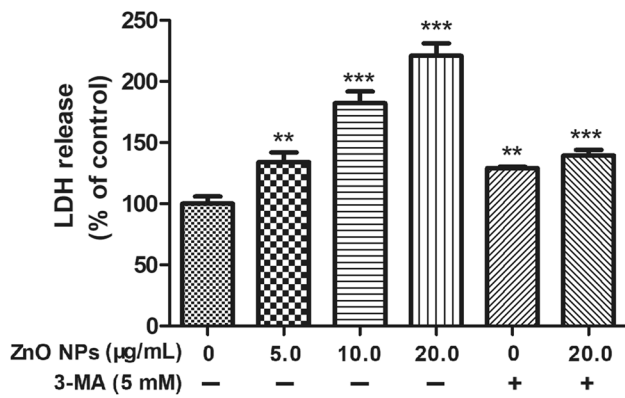


Fig. 4 Measurement of LDH release levels. RPMI8226 cells were treated with different concentrations (0, 5.0, 10.0, and 20.0 µg/mL) of ZnO NPs, 3-MA (5 mM), and ZnO NPs (20.0 µg/mL)+3-MA (5 mM) for 24 h, and then the LDH levels were measured using a commercial kit. Data were obtained from three independent experiments, and the results are presented as the mean ± SD. ***P* < 0.01 and ****P* < 0.001 compared with the control group

shows that compared to untreated cells, Becn1, Atg5, and Atg12 protein levels increased with increasing concentrations (0, 5.0, 10.0, and 20.0 µg/mL) of ZnO NPs (***P* < 0.01 and ****P* < 0.001 vs. relevant controls). The Becn1 protein level in RPMI8226 cells was increased from 49.32 pg/mg to 99.39, 103.73, and 118.88 pg/mg with concentration; Atg5 increased from 1.94 pg/mg to 3.62, 3.86, and 4.77 pg/mg with concentration; Atg12 increased from 1.55 pg/mg to 2.49, 2.54, and 3.90 pg/mg with concentration. The levels of these proteins increased in a concentration-dependent manner.

Enhancement of Light Chain 3 (LC3) Accumulation

Using the autophagy LC3 antibody-based kit, we discovered that following exposure to various concentrations (0, 5.0, 10.0, or 20.0 µg/mL) of ZnO NPs for 24 h, the intensity of LC3 was dramatically increased in RPMI8226 cells (Fig. 9A–D) in a dose-dependent manner (Fig. 9E, **P* < 0.05 and ****P* < 0.001 vs. control samples). The intensity of LC3 increased from 18.667 to 22.167, 29.000, and 50.800 with concentration.

Discussion

Nanotechnology is multidisciplinary and covers the fields of biology, engineering, chemistry, and physics. Due to their high biocompatibility, many forms of NPs have significant potential as drug/drug delivery carriers [43, 44]. As one of the most widely used NPs, ZnO NPs are effective for neurodegenerative diseases [45, 46] and cancer treatment [47, 48]. Here, we have evaluated, for the first time, the effects of ZnO NPs on MM using the human MM cell line RPMI8226. In this investigation, we noted that ZnO NPs could effectively inhibit the proliferation and promote the death of RPMI8226 cells in vitro in a dose- and time-dependent manner. ZnO NPs effectively increased LDH levels, enhanced MDC fluorescence intensity, and induced cell cycle arrest at the G2/M phase in RPMI8226 cells. Moreover, ZnO NPs also significantly increased the expression of Becn1, Atg5, and Atg12 at the mRNA and protein levels, enhanced the production of LC3, and triggered the autophagy signaling pathway.

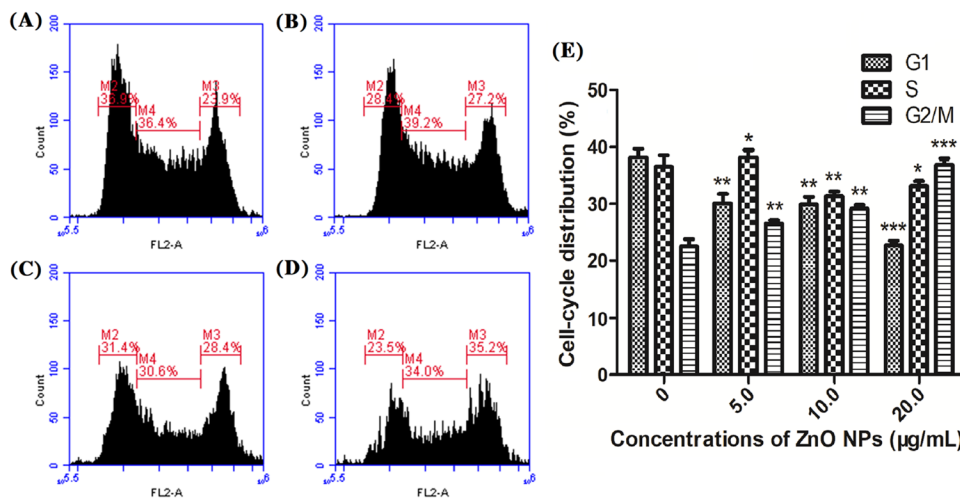
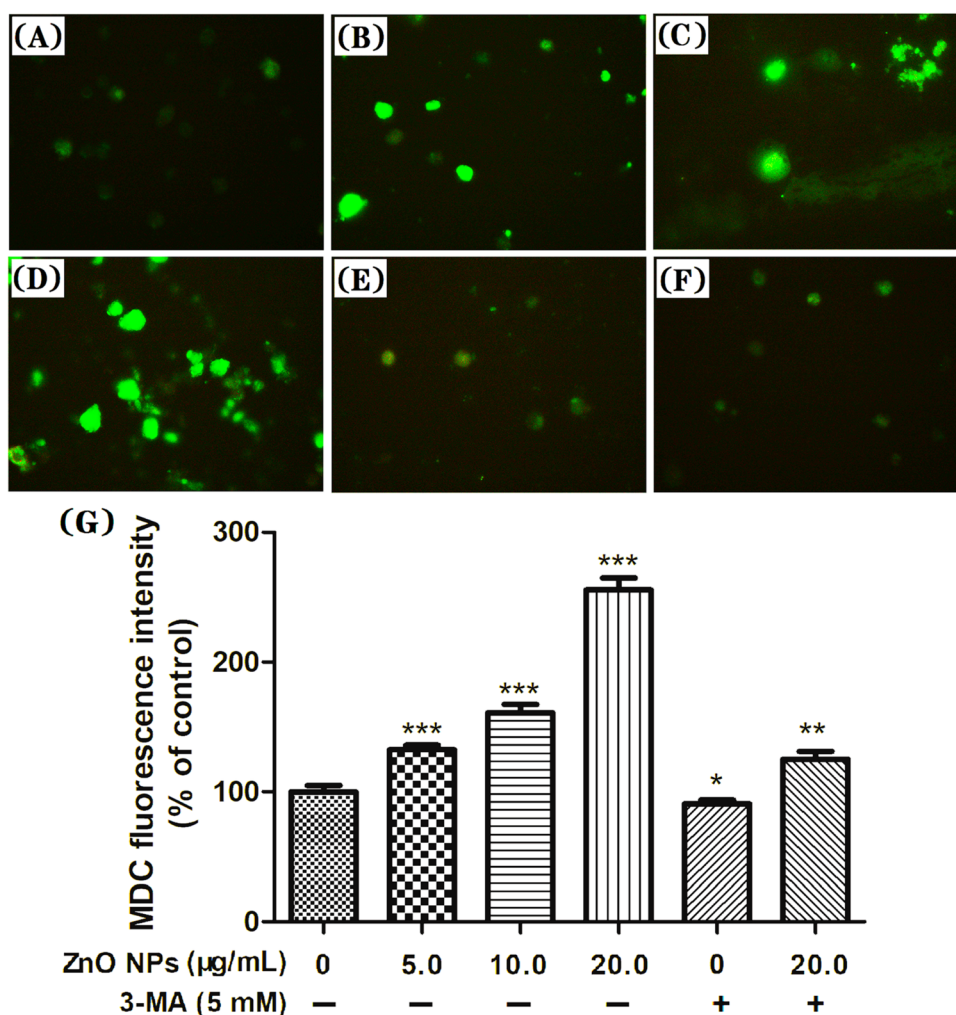


Fig. 5 Cell cycle distributions of RPMI8226 cells after treatment with different concentrations of ZnO NPs for 24 h. Cell cycle distribution was determined by flow cytometry (M2, G0/G1 phase; M3, G2/M phase; M4, S phase). (a) **A** Untreated cells; **B** cells treated with 5.0 µg/mL ZnO NPs; **C** cells treated with 10.0 µg/mL ZnO NPs; **D**

cells treated with 20.0 µg/mL ZnO NPs, and (b) **E** histogram analysis of the cell cycle phase distributions of human MM cells after treatment with different concentrations of ZnO NPs. Data were obtained from three independent experiments and are presented as the mean ± S.D., **P* < 0.05, ***P* < 0.01, and ****P* < 0.001

Fig. 6 After treatment with different concentrations (0, 5.0, 10.0, 20.0 $\mu\text{g}/\text{mL}$) of ZnO NPs, 3-MA (5 mM), and ZnO NPs (20.0 $\mu\text{g}/\text{mL}$) + 3-MA (5 mM) for 24 h, RPMI8226 cells were incubated with MDC and then measured using an Olympus fluorescence microscope. **A** Untreated cells; **B** cells treated with 5.0 $\mu\text{g}/\text{mL}$ ZnO NPs; **C** cells treated with 10.0 $\mu\text{g}/\text{mL}$ ZnO NPs; **D** cells treated with 20.0 $\mu\text{g}/\text{mL}$ ZnO NPs; **E** 3-MA (5 mM); **F** ZnO NPs (20.0 $\mu\text{g}/\text{mL}$) + 3-MA (5 mM); and **G** histogram analysis of MDC fluorescence intensity of RPMI8226 cells. Scale bars, 50 μm . The results are presented as the mean \pm SD of three independent experiments. * $P < 0.05$, ** $P < 0.01$, and. *** $P < 0.001$



In addition, the autophagy-induced effect of ZnO NPs on RPMI8226 cells was inhibited by 3-MA. Overall, ZnO NPs can trigger autophagy signaling in human MM cells and thus inhibit MM cell proliferation.

In our study, we performed MTT assays and we found that RPMI8226 cell viability exhibited a concentration- and time-dependent effect after treatment with ZnO NPs. The cell viability decreased gradually as the concentration of ZnO NPs incubated with the cells increased, and the culture time was extended (Fig. 2), demonstrating that ZnO NPs exert considerable cytotoxic effects on RPMI8226 cells. In addition, we found that the morphology of RPMI8226 cells changed significantly after exposure to ZnO NPs. As the concentration of ZnO NPs increased, the morphological changes in RPMI8226 cells became more severe (Fig. 3A–D). Due to their tiny size, ZnO NPs can diffuse into the nucleus and interact directly with DNA [49]. DNA damage can lead to impairment of normal cell function, which can result in cell death [50, 51]. Therefore, we hypothesize that ZnO NPs may disrupt the DNA structure and thus induce the death of RPMI8226 cells. Furthermore, our previous investigation

explored the effect of ZnO NPs on human peripheral blood mononuclear cells (PBMCs), and the results demonstrated that ZnO NPs showed little cytotoxic influence on PBMCs [24]. All these results indicate that ZnO NPs are significantly selective and cytotoxic to RPMI8226 cells.

LDH release is an important indicator of cell membrane integrity and is widely used in cytotoxicity assays [52]. Disruption of the cell membrane structure due to apoptosis or necrosis leads to the release of enzymes from the cell plasma into the culture medium. LDH is an enzyme that exists in the cytoplasm of living cells and is released outside the cell following damage to the cell membrane [53]. Thus, quantitative analysis of cytotoxicity can be achieved by detecting the levels of LDH released into the culture medium from cells with ruptured plasma membranes. In this study, the level of LDH released outside the cytoplasm indicates the integrity of the MM cell membrane. As shown in Fig. 4, after RPMI8226 cells were exposed to ZnO NPs, the LDH levels in the supernatant were highly elevated compared to the related control samples. Interestingly, 3-MA significantly inhibited ZnO NPs-induced LDH activity. Pandurangan et al.

Fig. 7 Gene expression of Becn1, Atg5, Atg12, and LC3. RPMI8226 cells were treated with different concentrations of ZnO NPs (5.0, 10.0, and 20.0 $\mu\text{g/mL}$) for 12 h, and the mRNA expression levels of Becn1, Atg5, Atg12, and LC3 were compared to those in untreated cells. **A** Becn1 mRNA level; **B** Atg5 mRNA level; **C** Atg12 mRNA level; and **D** LC3 mRNA level. The results are expressed as the mean \pm SD (standard deviation) of three independent experiments. * $P < 0.05$, ** $P < 0.01$, and *** $P < 0.001$

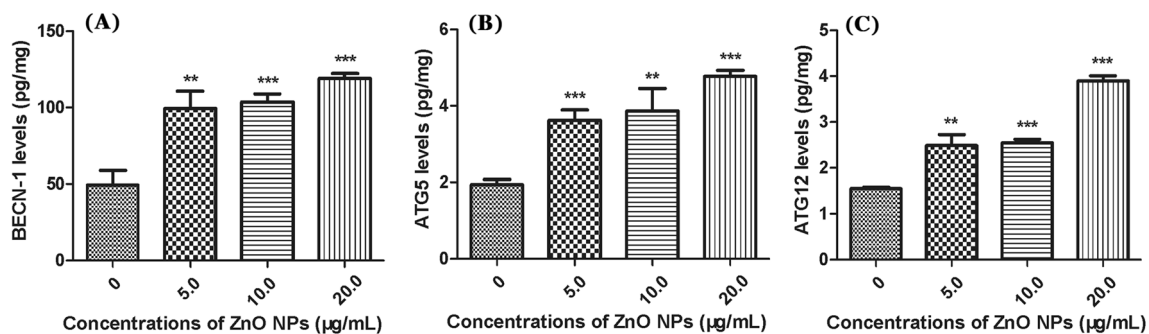
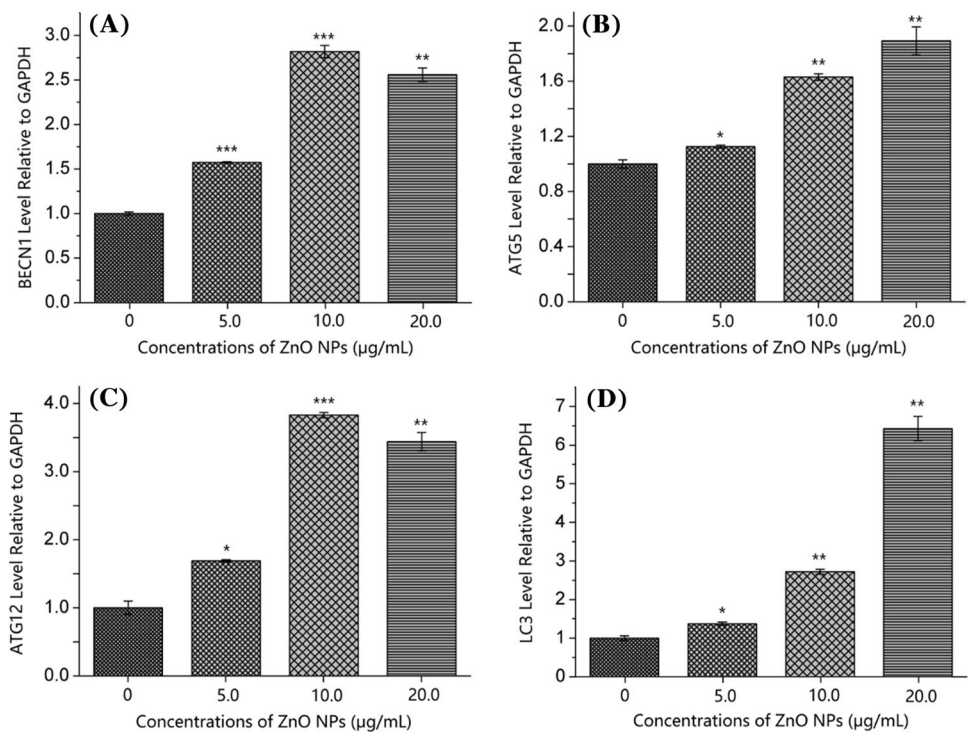


Fig. 8 Measurements of Becn1, Atg5, and Atg12 expression at the protein level in RPMI8226 cells. The cells were treated with different concentrations (0, 5.0, 10.0, and 20.0 $\mu\text{g/mL}$) of ZnO NPs for 24 h, and then the expression levels of Becn1, Atg5, and Atg12 at

the protein level were determined by ELISA. **A** Becn1 protein levels; **B** Atg5 protein levels; **C** Atg12 protein levels. Three independent experiments were performed. ** $P < 0.01$ and *** $P < 0.001$ vs. relevant control samples

showed that ZnO NPs increased LDH expression in C2C12 cells [54]. Jiang et al. observed that ZnO NPs increased LDH activity in lung tissue in a dose-dependent manner, while 3-MA down-regulated LDH activity [55]. Bai et al. found that ZnO NPs exert cytotoxic effects on human ovarian cancer cells in a manner that induces LDH release [29]. In conclusion, these results suggest that treatment with ZnO NPs can increase the permeability of cell membranes, thereby promoting the release of LDH into the culture medium and thus exerting a cytotoxic effect.

After decades of studies into the cell cycle and its importance in tumor progression, cell cycle arrest has been established as one of the most efficient tumor therapy

options [56]. In addition, it has been shown that inhibition of Golgi catabolism and related pathways leads to cell cycle arrest at the G2 phase [57]. The results of this study showed that RPMI8226 cells were arrested at the G2/M phase by ZnO NPs in a concentration-dependent manner (Fig. 5). Similarly, Boroumand et al. showed that ZnO NPs have the potential to arrest tumor cells at the G2/M phase [58]. Yin et al. demonstrated that ZnO NPs could lead to human tenon fibroblast cell cycle arrest at the G2/M phase and ultimately inhibit their proliferation [59]. These results are similar to our results. Our results show that ZnO NPs can cause cell cycle arrest in human MM cells. Cell cycle-arrested cells are unable to enter the

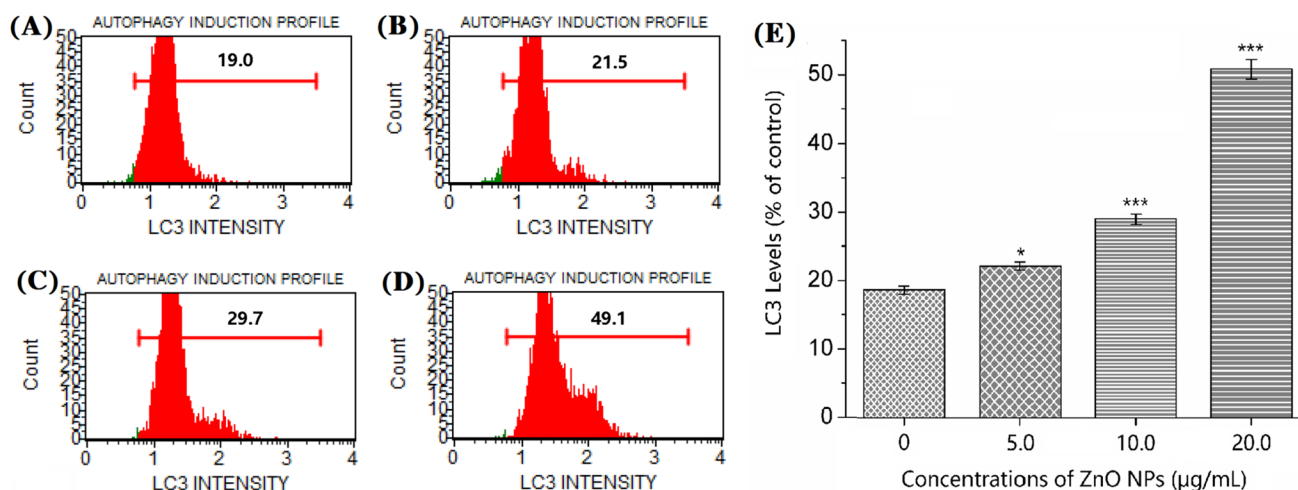


Fig. 9 Changes in LC3 intensity in RPMI8226 cells. The cells were treated with 0 µg/ml (A), 5.0 µg/ml (B), 10.0 µg/ml (C), or 20.0 µg/ml (D) ZnO NPs for 24 h and then treated with agents from the

Muse™ Autophagy LC3-antibody-based Kit. LC3 intensity was determined using a Muse™ Cell Analyzer. **E** Statistical analysis of LC3 intensity. * $P < 0.05$ and. *** $P < 0.001$ vs. control sample, $n = 3$

mitosis phase. Therefore, ZnO NPs may be a novel drug to block MM cell division.

Oxidative stress, hypoxia, and nutrient depletion can regulate the cell autophagic response [60]. The autophagy lysosomal degradation pathway, mediated by ATG, is essential for cellular, tissue, and organismal homeostasis [61]. Atg12 can bind to Atg5 via an enzymatic reaction. The Atg12-Atg5 conjugates function as E3 enzymes, promoting the lipidation of Atg8, which is essential for autophagosome formation during autophagy [62, 63]. Becn1, a major component of the class III phosphatidylinositol 3-kinase complex, mediates the formation and maturation of autophagosomes [64, 65]. In mammalian cells, LC3 is a universal marker protein for autophagic structures [66]. Here, the expression of Atg5, Atg12, LC3, and Becn1 was enhanced after treatment with ZnO NPs. MDC analysis also showed that autophagic vacuole formation increased with increasing concentrations of ZnO NPs, and ZnO NPs-induced autophagic vacuoles could be significantly inhibited by 3-MA, indicating that the autophagic pathway was activated. He et al. showed that ZnO NPs could induce human osteosarcoma cell autophagy accompanied by increased levels of Beclin-1, ATG5, and LC3 [67]. Guo et al. confirmed that ZnO NPs-triggered autophagy activation in human tenon fibroblasts by upregulating Atg5, Atg12, and Becn1 in human tenon fibroblasts [32]. All these results suggest that activation of the autophagic pathway mediated by ZnO NPs plays a particular role in human MM RPMI8226 cell death.

ZnO NPs exhibit the ability to preferentially kill tumor cells compared to normal cells. Studies have shown that ZnO NPs have selective cytotoxic effects on acute myeloid leukemia, hepatocellular carcinoma, lung adenocarcinoma, glioma, breast, and prostate cancer cells, whereas they have

no effect on normal PBMCs, astrocytes, or hepatocytes [22, 68, 69]. More interestingly, in vivo studies have shown no potential adverse effects on the liver, blood, immune system, or bone marrow of broiler chickens given diets containing ZnO NPs for long periods of time [70]. These studies reveal the safety of ZnO NPs in cancer treatment. In addition, although MM is a plasma cell carcinoma, it does not appear clinically in the circulation like other hematological disorders (leukemia/lymphoma). Instead, it forms solid lesions in the BM. As we did in vitro studies, we were unable to evaluate the ability of ZnO NPs to penetrate solid lesions and tumors. However, numerous in vivo studies have shown that ZnO NPs can reduce the weight and volume of tumors in the solid liver [71, 72], lung [73], stomach [74], breast [75], osteosarcoma [76], lymphoma [77], and solid Ehrlich carcinoma [78] and thus have anticancer potential.

The BM microenvironment (BMM) comprises a cellular compartment (e.g., osteoclasts, osteoblasts, stromal cells, and endothelial cells) and a noncellular compartment, including the extracellular matrix and the liquid milieu (containing cytokines, growth factors, and chemokines) [79, 80]. Almost all MM plasma cells are strictly dependent on their interaction with components of the BMM [81]. Studies have shown that bone marrow mesenchymal stem cells (BM-MSCs) are involved in the construction of the MM microenvironment and are closely related to the growth of MM cells and bone destruction [82]. Normal bone remodeling is based on the balance between bone formation by osteoblasts (OBs) and bone degradation by osteoclasts (OCs) [83]. MM patients develop bone damage due to the imbalance of this homeostasis. The interaction between the ZnO NPs-induced autophagic effect and the BMM needs to be further investigated.

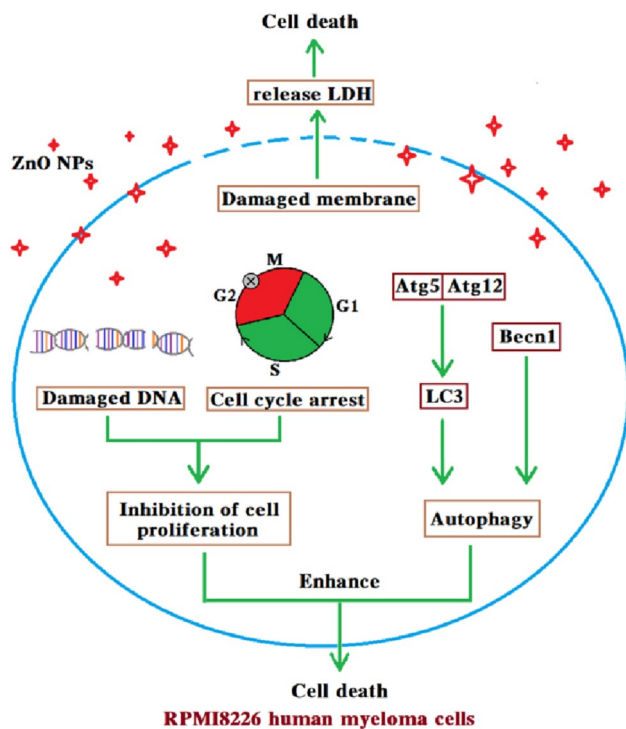


Fig. 10 A schematic illustration of ZnO NPs inducing RPMI8226 human MM cell death by triggering autophagy

As summarized in Fig. 10, exposure of RPMI8226 cells to ZnO NPs can significantly stimulate the autophagic signaling pathway, limiting RPMI8226 cell proliferation and inducing cell death.

Conclusions

Overall, ZnO NPs exert a dose-dependent inhibitory effect on the human MM cell line RPMI8226, increase LDH levels and MDC fluorescence intensity, and induce cell cycle arrest at the G2/M phase. In addition, ZnO NPs significantly increased the expression of Becn1, Atg5, Atg12, and LC3 at the mRNA and protein levels, thereby activating the autophagic signaling pathway. Our findings pave the way for a better understanding of the molecular mechanisms by which ZnO NPs inhibit RPMI8226 cell proliferation by activating the autophagic signaling pathway. Animal studies should be performed next to confirm the therapeutic effects of ZnO NPs on MM.

Author Contribution Zonghong Li: conceptualization, data curation, formal analysis, investigation, methodology, writing—original draft. Xuwei Yin: conceptualization, data curation, formal analysis, investigation, methodology, writing—original draft. Chunyi Lyu: software, supervision, validation. Jingyi Wang: data curation, investigation, methodology. Kui Liu: investigation, methodology, validation. Siyuan

Cui: investigation, methodology, validation. Shumin Ding: investigation, validation. Yingying Wang: investigation, visualization. Jinxin Wang: investigation, visualization. Dadong Guo: conceptualization, resources, supervision, writing—review and editing. Ruirong Xu: conceptualization, funding acquisition, project administration, writing—review & editing. All authors have read and agreed to the published version of the manuscript.

Funding This study was funded by the National Natural Science Foundation of China (81974547) and the Natural Science Foundation of Shandong Province (ZR2019PH018, ZR2020KH023).

Data Availability The data sets used and analyzed during the current study are available from the corresponding author on reasonable request.

Declarations

Ethics Approval and Consent to Participate Not applicable.

Consent for Publication All listed authors have actively participated in the study and have read and approved the submitted manuscript.

Competing Interests The authors declare no competing interests.

References

- Rajkumar SV, Kumar S (2020) Multiple myeloma current treatment algorithms. *Blood Cancer J* 10(9):94. <https://doi.org/10.1038/s41408-020-00359-2>
- Kumar SK, Rajkumar V, Kyle RA et al (2017) Multiple myeloma. *Nat Rev Dis Primers* 3:17046. <https://doi.org/10.1038/nrdp.2017.46>
- Wang S, Xu L, Feng J, Liu Y, Liu L, Wang J, Liu J, Huang X, Gao P, Lu J, Zhan S (2020) Prevalence and incidence of multiple myeloma in urban area in China: a national population-based analysis. *Front Oncol* 24(9):1513. <https://doi.org/10.3389/fonc.2019.01513>
- Liu W, Liu J, Song Y, Wang X, Zhou M, Wang L, Ma J, Zhu J, Union for China Leukemia Investigators of the Chinese Society of Clinical Oncology, Union for China Lymphoma Investigators of the Chinese Society of Clinical Oncology (2019) Mortality of lymphoma and myeloma in China, 2004–2017: an observational study. *J Hematol Oncol* 12(1):22. <https://doi.org/10.1186/s13045-019-0706-9>
- Siegel RL, Miller KD, Jemal A (2020) Cancer statistics, 2020. *CA Cancer J Clin* 70(1):7–30. <https://doi.org/10.3322/caac.21590>
- Moreau P (2017) How I treat myeloma with new agents. *Blood* 130(13):1507–1513. <https://doi.org/10.1182/blood-2017-05-743203>
- Gonzalez-Santamarta M, Quinet G, Reyes-Garau D, Sola B, Roué G, Rodriguez MS (2020) Resistance to the proteasome inhibitors: lessons from multiple myeloma and mantle cell lymphoma. *Adv Exp Med Biol* 1233:153–174. https://doi.org/10.1007/978-3-030-38266-7_6
- Corre J, Munshi NC, Avet-Loiseau H (2021) Risk factors in multiple myeloma: is it time for a revision? *Blood* 137(1):16–19. <https://doi.org/10.1182/blood.2019004309>
- Nakamura K, Smyth MJ, Martinet L (2020) Cancer immunoediting and immune dysregulation in multiple myeloma. *Blood* 136(24):2731–2740. <https://doi.org/10.1182/blood.2020006540>
- Chari A, Martinez-Lopez J, Mateos MV, Bladé J, Benboubker L, Oriol A, Arnulf B, Rodriguez-Otero P, Pineiro L, Jakubowiak A,

- de Boer C, Wang J, Clemens PL, Ukropec J, Schechter J, Lonial S, Moreau P (2019) Daratumumab plus carfilzomib and dexamethasone in patients with relapsed or refractory multiple myeloma. *Blood* 134(5):421–431. <https://doi.org/10.1182/blood.201900722>
11. Pawlyn C, Davies FE (2019) Toward personalized treatment in multiple myeloma based on molecular characteristics. *Blood* 133(7):660–675. <https://doi.org/10.1182/blood-2018-09-825331>
 12. Thorsteinsdottir S, Gislason G, Aspelund T, Sverrisdottir I, Landgren O, Turesson I, Björkholm M, Kristinsson SY (2020) Fractures and survival in multiple myeloma: results from a population-based study. *Haematologica* 105(4):1067–1073. <https://doi.org/10.3324/haematol.2019.230011>
 13. Goodman AM, Kim MS, Prasad V (2021) Persistent challenges with treating multiple myeloma early. *Blood* 137(4):456–458. <https://doi.org/10.1182/blood.2020009752>
 14. Li B, Xu H, Li Z, Yao M, Xie M, Shen H, Shen S, Wang X, Jin Y (2012) Bypassing multidrug resistance in human breast cancer cells with lipid/polymer particle assemblies. *Int J Nanomedicine* 7:187–197. <https://doi.org/10.2147/IJN.S27864>
 15. Rasmussen JW, Martinez E, Louka P, Wingett DG (2010) Zinc oxide nanoparticles for selective destruction of tumor cells and potential for drug delivery applications. *Expert Opin Drug Deliv* 7(9):1063–1077. <https://doi.org/10.1517/17425247.2010.502560>
 16. Bai Aswathanarayan J, Rai Vittal R, Muddegowda U (2018) Anticancer activity of metal nanoparticles and their peptide conjugates against human colon adenorectal carcinoma cells. *Artif Cells Nanomed Biotechnol* 46(7):1444–1451. <https://doi.org/10.1080/21691401.2017.1373655>
 17. Zhang Y, Nayak TR, Hong H, Cai W (2013) Biomedical applications of zinc oxide nanomaterials. *Curr Mol Med* 13(10):1633–1645. <https://doi.org/10.2174/156652401366613111130058>
 18. Mishra PK, Mishra H, Ekielski A, Talegaonkar S, Vaidya B (2017) Zinc oxide nanoparticles: a promising nanomaterial for biomedical applications. *Drug Discov Today* 22(12):1825–1834. <https://doi.org/10.1016/j.drudis.2017.08.006>
 19. Guo D, Wu C, Jiang H, Li Q, Wang X, Chen B (2008) Synergistic cytotoxic effect of different sized ZnO nanoparticles and daunorubicin against leukemia cancer cells under UV irradiation. *J Photochem Photobiol B* 93(3):119–126. <https://doi.org/10.1016/j.jphotobiol.2008.07.009>
 20. Tang KS (2019) The current and future perspectives of zinc oxide nanoparticles in the treatment of diabetes mellitus. *Life Sci* 239:117011. <https://doi.org/10.1016/j.lfs.2019.117011>
 21. Lallo da Silva B, Caetano BL, Chiari-Andréo BG, Pietro RCLR, Chiavacci LA (2019) Increased antibacterial activity of ZnO nanoparticles: influence of size and surface modification. *Colloids Surf B Biointerfaces* 177:440–447. <https://doi.org/10.1016/j.colsurfb.2019.02.013>
 22. Akhtar MJ, Ahamed M, Kumar S, Khan MM, Ahmad J, Alrokayan SA (2012) Zinc oxide nanoparticles selectively induce apoptosis in human cancer cells through reactive oxygen species. *Int J Nanomedicine* 7:845–857. <https://doi.org/10.2147/IJN.S29129>
 23. Sasidharan A, Chandran P, Menon D, Raman S, Nair S, Koyakutty M (2011) Rapid dissolution of ZnO nanocrystals in acidic cancer microenvironment leading to preferential apoptosis. *Nanoscale* 3(9):3657–3669. <https://doi.org/10.1039/c1nr10272a>
 24. Li Z, Guo D, Yin X, Ding S, Shen M, Zhang R, Wang Y, Xu R (2020) Zinc oxide nanoparticles induce human multiple myeloma cell death via reactive oxygen species and Cyt-C/Apaf-1/Caspase-9/Caspase-3 signaling pathway in vitro. *Biomed Pharmacother* 122:109712. <https://doi.org/10.1016/j.biopha.2019.109712>
 25. Zeng X, Ju D (2018) Hedgehog signaling pathway and autophagy in cancer. *Int J Mol Sci* 19(8):2279. <https://doi.org/10.3390/ijms19082279>
 26. Yu L, Chen Y, Tooze SA (2018) Autophagy pathway: cellular and molecular mechanisms. *Autophagy* 14(2):207–215. <https://doi.org/10.1080/15548627.2017.1378838>
 27. Tsujimoto Y, Shimizu S (2005) Another way to die: autophagic programmed cell death. *Cell Death Differ* 12(Suppl 2):1528–1534. <https://doi.org/10.1038/sj.cdd.4401777>
 28. Amaravadi RK, Thompson CB (2007) The roles of therapy-induced autophagy and necrosis in cancer treatment. *Clin Cancer Res* 13(24):7271–7279. <https://doi.org/10.1158/1078-0432.CCR-07-1595>
 29. Bai DP, Zhang XF, Zhang GL, Huang YF, Gurunathan S (2017) Zinc oxide nanoparticles induce apoptosis and autophagy in human ovarian cancer cells. *Int J Nanomedicine* 5(12):6521–6535. <https://doi.org/10.2147/IJN.S140071>
 30. Hackenberg S, Scherzed A, Gohla A, Technau A, Froelich K, Ginzkey C, Koehler C, Burghartz M, Hagen R, Kleinsasser N (2014) Nanoparticle-induced photocatalytic head and neck squamous cell carcinoma cell death is associated with autophagy. *Nanomedicine (Lond)* 9(1):21–33. <https://doi.org/10.2217/nmm.13.41>
 31. Liu J, Kang Y, Yin S, Chen A, Wu J, Liang H, Shao L (2019) Key role of microtubule and its acetylation in a zinc oxide nanoparticle-mediated lysosome-autophagy system. *Small* 15(25):e1901073. <https://doi.org/10.1002/sml.201901073>
 32. Guo D, Wang Z, Guo L, Yin X, Li Z, Zhou M, Li T, Chen C, Bi H (2021) Zinc oxide nanoparticle-triggered oxidative stress and autophagy activation in human tenon fibroblasts. *Eur J Pharmacol* 907:174294. <https://doi.org/10.1016/j.ejphar.2021.174294>
 33. He G, Ma Y, Zhu Y, Yong L, Liu X, Wang P, Liang C, Yang C, Zhao Z, Hai B, Pan X, Liu Z, Liu X, Mao C (2018) Cross talk between autophagy and apoptosis contributes to ZnO nanoparticle-induced human osteosarcoma cell death. *Adv Healthc Mater* 7(17):e1800332. <https://doi.org/10.1002/adhm.201800332>
 34. Yin X, Li Z, Lyu C, Wang Y, Ding S, Ma C, Wang J, Cui S, Wang J, Guo D, Xu R (2022) Induced effect of zinc oxide nanoparticles on human acute myeloid leukemia cell apoptosis by regulating mitochondrial division. *IUBMB Life*. <https://doi.org/10.1002/iub.2615>
 35. Kadow S, Schumacher F, Kramer M, Hessler G, Scholtysik R, Oubari S, Johansson P, Hüttmann A, Reinhardt HC, Kleuser B, Zoratti M, Mattarei A, Szabò I, Gulbins E, Carpinteiro A (2022) Mitochondrial Kv1.3 channels as target for treatment of multiple myeloma. *Cancers (Basel)* 14(8):1955. <https://doi.org/10.3390/cancers14081955>
 36. Jiang J, Ge H, Yang J, Qiao Y, Xu X, Geng Y (2022) CircRNA protein tyrosine phosphatase receptor type a suppresses proliferation and induces apoptosis of lung adenocarcinoma cells via regulation of microRNA-582-3p. *Bioengineered* 13(5):12182–12192. <https://doi.org/10.1080/21655979.2022.2073319>
 37. Li L, Wang H, Li H, Lu X, Gao Y, Guo X (2022) Long non-coding RNA BACE1-antisense transcript plays a critical role in Parkinson's disease via microRNA-214-3p/Cell death-inducing p53-target protein 1 axis. *Bioengineered* 13(4):10889–10901. <https://doi.org/10.1080/21655979.2022.2066750>
 38. Jaouadi O, Limam I, Abdelkarim M et al (2021) 5,6-Epoxycholesterol isomers induce oxiaoptophagy in myeloma cells. *Cancers (Basel)* 13(15):3747. <https://doi.org/10.3390/cancers13153747>
 39. Song Y, Yu J, Li L, Wang L, Dong L, Xi G, Lu YJ, Li Z (2022) Luteolin impacts deoxyribonucleic acid repair by modulating the mitogen-activated protein kinase pathway in colorectal cancer. *Bioengineered* 13(4):10998–11011. <https://doi.org/10.1080/21655979.2022.2066926>
 40. Li W, Zhang S, Liu J, Liu Y, Liang Q (2019) Vitamin K2 stimulates MC3T3-E1 osteoblast differentiation and mineralization through autophagy induction. *Mol Med Rep* 19(5):3676–3684. <https://doi.org/10.3892/mmr.2019.10040>

41. Nemati S, Pazoki H, Mohammad Rahimi H et al (2021) Toxoplasma gondii profilin and tachyzoites RH strain may manipulate autophagy via downregulating Atg5 and Atg12 and upregulating Atg7. *Mol Biol Rep* 48(10):7041–7047. <https://doi.org/10.1007/s11033-021-06667-5>
42. Chen X, Tong G, Fan J, Shen Y, Wang N, Gong W, Hu Z, Zhu K, Li X, Jin L, Cong W, Xiao J, Zhu Z (2022) FGF21 promotes migration and differentiation of epidermal cells during wound healing via SIRT1-dependent autophagy. *Br J Pharmacol* 179(5):1102–1121. <https://doi.org/10.1111/bph.15701>
43. Berdiaki A, Perisynaki E, Stratidakis A, Kulikov PP, Kuskov AN, Stivaktakis P, Henrich-Noack P, Luss AL, Shtilman MM, Tzanakakis GN, Tsatsakis A, Nikitovic D (2020) Assessment of amphiphilic poly-N-vinylpyrrolidone nanoparticles' biocompatibility with endothelial cells *in vitro* and delivery of an anti-inflammatory drug. *Mol Pharm* 17(11):4212–4225. <https://doi.org/10.1021/acs.molpharmaceut.0c00667>
44. Tsatsakis A, Stratidakis AK, Goryachaya AV, Tzatzarakis MN, Stivaktakis PD, Docea AO, Berdiaki A, Nikitovic D, Velonia K, Shtilman MI, Rizos AK, Kuskov AN (2019) In vitro blood compatibility and in vitro cytotoxicity of amphiphilic poly-N-vinylpyrrolidone nanoparticles. *Food Chem Toxicol* 127:42–52. <https://doi.org/10.1016/j.fct.2019.02.041>
45. Ashraf JM, Ansari MA, Fatma S, Abdullah SMS, Iqbal J, Madkhali A, Hamali AH, Ahmad S, Jerah A, Echeverria V, Barreto GE, Ashraf GM (2018) Inhibiting effect of zinc oxide nanoparticles on advanced glycation products and oxidative modifications: a potential tool to counteract oxidative stress in neurodegenerative diseases. *Mol Neurobiol* 55(9):7438–7452. <https://doi.org/10.1007/s12035-018-0935-x>
46. Lai L, Jiang X, Han S, Zhao C, Du T, Rehman FU, Zheng Y, Li X, Liu X, Jiang H, Wang X (2017) In vivo biosynthesized zinc and iron oxide nanoclusters for high spatiotemporal dual-modality bioimaging of Alzheimer's disease. *Langmuir* 33(36):9018–9024. <https://doi.org/10.1021/acs.langmuir.7b01516>
47. Ye DX, Ma YY, Zhao W, Cao HM, Kong JL, Xiong HM, Møhwald H (2016) ZnO-based nanoplatfoms for labeling and treatment of mouse tumors without detectable toxic side effects. *ACS Nano* 10(4):4294–4300. <https://doi.org/10.1021/acs.nano.5b07846>
48. Paino IM, Goncalves JF, Souza FL, Zucolotto V (2016) Zinc oxide flower-like nanostructures that exhibit enhanced toxicology effects in cancer cells. *ACS Appl Mater Interfaces*. 8(48):32699–32705. <https://doi.org/10.1021/acsami.6b11950>
49. Reshma VG (2017) Mohanan PV Cellular interactions of zinc oxide nanoparticles with human embryonic kidney (HEK 293) cells. *Colloids Surf B Biointerfaces*. 157:182–190. <https://doi.org/10.1016/j.colsurfb.2017.05.069>
50. Chen M, von Mikecz A (2005) Formation of nucleoplasmic protein aggregates impairs nuclear function in response to SiO₂ nanoparticles. *Exp Cell Res* 305(1):51–62. <https://doi.org/10.1016/j.yexcr.2004.12.021>
51. Sharma V, Singh SK, Anderson D, Tobin DJ, Dhawan A (2011) Zinc oxide nanoparticle induced genotoxicity in primary human epidermal keratinocytes. *J Nanosci Nanotechnol* 11(5):3782–3788. <https://doi.org/10.1166/jnn.2011.4250>
52. Kwan YP, Saito T, Ibrahim D et al (2016) Evaluation of the cytotoxicity, cell-cycle arrest, and apoptotic induction by Euphorbia hirta in MCF-7 breast cancer cells. *Pharm Biol* 54(7):1223–1236. <https://doi.org/10.3109/13880209.2015.1064451>
53. Zhao D, Sun Y, Tan Y et al (2018) Short-duration swimming exercise after myocardial infarction attenuates cardiac dysfunction and regulates mitochondrial quality control in aged mice. *Oxid Med Cell Longev*. 2018:4079041. <https://doi.org/10.1155/2018/4079041>
54. Pandurangan M, Kim DH (2015) ZnO nanoparticles augment ALT, AST, ALP and LDH expressions in C2C12 cells. *Saudi J Biol Sci* 22(6):679–684. <https://doi.org/10.1016/j.sjbs.2015.03.013>
55. Jiang X, Tang Q, Zhang J et al (2018) Autophagy-dependent release of zinc ions is critical for acute lung injury triggered by zinc oxide nanoparticles. *Nanotoxicology* 12(9):1068–1091. <https://doi.org/10.1080/17435390.2018.1513094>
56. Otto T, Sicinski P (2017) Cell cycle proteins as promising targets in cancer therapy. *Nat Rev Cancer* 17(2):93–115. <https://doi.org/10.1038/nrc.2016.138>
57. Cervigni RI, Bonavita R, Barretta ML, Spano D, Ayala I, Nakamura N, Corda D, Colanzi A (2015) JNK2 controls fragmentation of the Golgi complex and the G2/M transition through phosphorylation of GRASP65. *J Cell Sci* 128(12):2249–2260. <https://doi.org/10.1242/jcs.164871>
58. Boroumand Moghaddam A, Moniri M, Azizi S, Abdul Rahim R, Bin Ariff A, Navaderi M, Mohamad R (2017) Eco-friendly formulated zinc oxide nanoparticles: induction of cell cycle arrest and apoptosis in the MCF-7 cancer cell line. *Genes (Basel)* 8(10):281. <https://doi.org/10.3390/genes8100281>
59. Yin X, Li Q, Wei H, Chen N, Wu S, Yuan Y, Liu B, Chen C, Bi H, Guo D (2019) Zinc oxide nanoparticles ameliorate collagen lattice contraction in human tenon fibroblasts. *Arch Biochem Biophys* 15(669):1–10. <https://doi.org/10.1016/j.abb.2019.05.016>
60. Siedlecka-Kroplewska K, Wozniak M, Kmiec Z (2019) The wine polyphenol resveratrol modulates autophagy and induces apoptosis in MOLT-4 and HL-60 human leukemia cells. *J Physiol Pharmacol* 70(6). <https://doi.org/10.26402/jpp.2019.6.02>
61. Levine B, Kroemer G (2019) Biological functions of autophagy genes: a disease perspective. *Cell* 176(1–2):11–42. <https://doi.org/10.1016/j.cell.2018.09.048>
62. Noda NN, Inagaki F (2015) Mechanisms of autophagy. *Annu Rev Biophys* 44:101–122. <https://doi.org/10.1146/annurev-biophys-060414-034248>
63. Noda NN, Fujioka Y, Hanada T, Ohsumi Y, Inagaki F (2013) Structure of the Atg12-Atg5 conjugate reveals a platform for stimulating Atg8-PE conjugation. *EMBO Rep* 14(2):206–211. <https://doi.org/10.1038/embor.2012.208>
64. Mei Y, Glover K, Su M, Sinha SC (2016) Conformational flexibility of BECN1: essential to its key role in autophagy and beyond. *Protein Sci* 25(10):1767–1785. <https://doi.org/10.1002/pro.2984>
65. Choubey V, Cagalinec M, Liiv J, Safiulina D, Hickey MA, Kuum M, Liiv M, Anwar T, Eskelinen EL, Kaasik A (2014) BECN1 is involved in the initiation of mitophagy: it facilitates PARK2 translocation to mitochondria. *Autophagy* 10(6):1105–1119. <https://doi.org/10.4161/auto.28615>
66. Kimura S, Fujita N, Noda T, Yoshimori T (2009) Monitoring autophagy in mammalian cultured cells through the dynamics of LC3. *Methods Enzymol* 452:1–12. [https://doi.org/10.1016/S0076-6879\(08\)03601-X](https://doi.org/10.1016/S0076-6879(08)03601-X)
67. He G, Pan X, Liu X, Zhu Y, Ma Y, Du C, Liu X, Mao C (2020) HIF-1 α -mediated mitophagy determines ZnO nanoparticle-induced human osteosarcoma cell death both in vitro and in vivo. *ACS Appl Mater Interfaces* 12(43):48296–48309. <https://doi.org/10.1021/acsami.0c12139>
68. Altunbek M, Keleştemur S, Baran G, Çulha M (2018) Role of modification route for zinc oxide nanoparticles on protein structure and their effects on glioblastoma cells. *Int J Biol Macromol* 118(Pt A):271–278. <https://doi.org/10.1016/j.ijbiomac.2018.06.059>
69. Premanathan M, Karthikeyan K, Jeyasubramanian K, Manivannan G (2011) Selective toxicity of ZnO nanoparticles toward Gram-positive bacteria and cancer cells by apoptosis through lipid peroxidation. *Nanomedicine* 7(2):184–192. <https://doi.org/10.1016/j.nano.2010.10.001>
70. Mahmoud MAM, Yahia D, Abdel-Magiud DS, Darwish MHA, Abd-Elkareem M, Mahmoud UT (2021) Broiler welfare is

- preserved by long-term low-dose oral exposure to zinc oxide nanoparticles: preliminary study. *Nanotoxicology* 15(5):605–620. <https://doi.org/10.1080/17435390.2021.1905099>
71. Hassan HF, Mansour AM, Abo-Youssef AM, Elsadek BE, Messiha BA (2017) Zinc oxide nanoparticles as a novel anticancer approach; in vitro and in vivo evidence. *Clin Exp Pharmacol Physiol* 44(2):235–243. <https://doi.org/10.1111/1440-1681.12681>
 72. RahimiKalateh Shah Mohammad G, Seyedi SMR, Karimi E, Homayouni-Tabrizi M (2019) The cytotoxic properties of zinc oxide nanoparticles on the rat liver and spleen, and its anticancer impacts on human liver cancer cell lines. *J Biochem Mol Toxicol* 33(7):e22324. <https://doi.org/10.1002/jbt.22324>
 73. Tanino R, Amano Y, Tong X, Sun R, Tsubata Y, Harada M, Fujita Y, Isobe T (2020) Anticancer activity of ZnO nanoparticles against human small-cell lung cancer in an orthotopic mouse model. *Mol Cancer Ther* 19(2):502–512. <https://doi.org/10.1158/1535-7163.MCT-19-0018>
 74. Miao YH, Mao LP, Cai XJ, Mo XY, Zhu QQ, Yang FT, Wang MH (2021) Zinc oxide nanoparticles reduce the chemoresistance of gastric cancer by inhibiting autophagy. *World J Gastroenterol* 27(25):3851–3862. <https://doi.org/10.3748/wjg.v27.i25.3851>
 75. Mahdizadeh R, Homayouni-Tabrizi M, Neamati A, Seyedi SMR, TavakkolAfshari HS (2019) Green synthesized-zinc oxide nanoparticles, the strong apoptosis inducer as an exclusive anticancer agent in murine breast tumor model and human breast cancer cell lines (MCF7). *J Cell Biochem* 120(10):17984–17993. <https://doi.org/10.1002/jcb.29065>
 76. Pan X, He G, Hai B, Liu Y, Bian L, Yong L, Zhang H, Yang C, Du C, Mao T, Ma Y, Jia F, Dou X, Zhai S, Liu X (2021) VPS34 regulates dynamin to determine the endocytosis of mitochondria-targeted zinc oxide nanoparticles in human osteosarcoma cells. *J Mater Chem B* 9(11):2641–2655. <https://doi.org/10.1039/d1tb00226k>
 77. Raajshree RK, Brindha D (2018) In vivo anticancer activity of biosynthesized zinc oxide nanoparticle using *Turbinaria conoides* on a Dalton's lymphoma ascites mice model. *J Environ Pathol Toxicol Oncol* 37(2):103–115. <https://doi.org/10.1615/JEnvironPatholToxicolOncol.2018025086>
 78. Sayed HM, Said MM, Morcos NYS, El Gawish MA, Ismail AFM (2021) Antitumor and radiosensitizing effects of zinc oxide-caffeic acid nanoparticles against solid Ehrlich carcinoma in female mice. *Integr Cancer Ther* 20:15347354211021920. <https://doi.org/10.1177/15347354211021920>
 79. Kawano Y, Moschetta M, Manier S et al (2015) Targeting the bone marrow microenvironment in multiple myeloma. *Immunol Rev* 263(1):160–172. <https://doi.org/10.1111/imr.12233>
 80. Manier S, Sacco A, Leleu X, Ghobrial IM, Roccaro AM (2012) Bone marrow microenvironment in multiple myeloma progression. *J Biomed Biotechnol* 2012:157496. <https://doi.org/10.1155/2012/157496>
 81. Rajkumar SV (2016) Multiple myeloma: 2016 update on diagnosis, risk-stratification, and management. *Am J Hematol* 91(7):719–734. <https://doi.org/10.1002/ajh.24402>
 82. Xu S, De Veirman K, De Becker A, Vanderkerken K, Van Riet I (2018) Mesenchymal stem cells in multiple myeloma: a therapeutic tool or target? *Leukemia* 32(7):1500–1514. <https://doi.org/10.1038/s41375-018-0061-9>
 83. Terpos E, Ntanasis-Stathopoulos I, Gavriatopoulou M, Dimopoulos MA (2018) Pathogenesis of bone disease in multiple myeloma: from bench to bedside. *Blood Cancer J* 8(1):7. <https://doi.org/10.1038/s41408-017-0037-4>

Publisher's Note Springer Nature remains neutral with regard to jurisdictional claims in published maps and institutional affiliations.

Springer Nature or its licensor (e.g. a society or other partner) holds exclusive rights to this article under a publishing agreement with the author(s) or other rightsholder(s); author self-archiving of the accepted manuscript version of this article is solely governed by the terms of such publishing agreement and applicable law.

Authors and Affiliations

Zonghong Li¹ · Xuewei Yin¹ · Chunyi Lyu¹ · Jingyi Wang² · Kui Liu² · Siyuan Cui² · Shumin Ding² · Yingying Wang² · Jinxin Wang² · Dadong Guo³ · Ruirong Xu^{2,4,5}

✉ Dadong Guo
dadonggene@163.com

✉ Ruirong Xu
shandongxuruirong@163.com

¹ Shandong University of Traditional Chinese Medicine, Jinan, Shandong Province, China

² Department of Hematology, the Affiliated Hospital of Shandong University of Traditional Chinese Medicine, No. 16369#, Jingshi Road, Jinan 250014, Shandong Province, China

³ Shandong Provincial Key Laboratory of Integrated Traditional Chinese and Western Medicine for Prevention

and Therapy of Ocular Diseases, Shandong Academy of Eye Disease Prevention and Therapy, Affiliated Eye Hospital of Shandong, University of Traditional Chinese Medicine, No. 48#, Yingxiongshan Road, Jinan, Shandong Province, China

⁴ Key Laboratory of Integrated Traditional Chinese and Western Medicine for Hematology, Health Commission of Shandong Province, Jinan 250014, China

⁵ Institute of Hematology, Shandong University of Traditional Chinese Medicine, Jinan 250014, China